Ann. Rev. Astron. Astrophys. 1979. 17: 275–308

STELLAR WINDS

Joseph P. Cassinelli
Washburn Observatory, University of Wisconsin, Madison, Wisconsin 53706

1 INTRODUCTION

This review is concerned with theories explaining the continual expansion of the outer atmospheric layers of luminous early- and late-type stars. For these stars the winds are sufficiently massive to be optically thick in the opacity of strong resonance lines and in certain continua. Thus, the winds are detectable through the emergent stellar spectra. Analyses of the strengths of the spectral features indicate that the stars are losing mass at a rate as high as 10^{-5} $M_\odot$/yr. The shortward displacement of absorption lines yields information concerning the velocities of the winds. The terminal velocities are large for the early-type stars, 600–3500 km/sec, but are small for the K and M stars, 10–100 km/sec.

Much of the interest in stellar winds in the past decade was stimulated by the discovery of the high velocity outflows from O and B supergiants by Morton (1967) and his co-workers (Morton, Jenkins & Brooks 1969). Their rocket-ultraviolet observations showed broad P Cygni-shaped profiles of lines of moderate stages of ionization, such as C^{+3}. The ionization stages and the high flow velocities could not be explained by a simple extrapolation of solar wind theory, and this led to the development of radiatively driven wind theories. In contrast, the winds from evolved K and M stars are detected through narrow P Cygni lines in the cores of strong Fraunhofer lines, and the velocities are well below the photospheric escape speeds. Deutsch (1956) proved that the features represent an actual mass loss from the stars by showing that the expansion extends to several hundred stellar radii where the rate of expansion exceeds the local escape speed.

Although most of the recent work on stellar winds concerns giants and supergiants, there is indirect evidence for winds from stars on the main sequence. For example, stars with spectral type later than F5V have low rotation speeds (Kraft 1967), which can be explained as a consequence of loss of angular momentum through the coupling of the stellar magnetic field with the expanding coronal plasma. The mechanism for the mass and

0066-4146/79/0915-0275$01.00

angular momentum loss of these stars is probably the same as that for the sun, and is not considered in this review. The solar wind is treated in the books by Parker (1963), Brandt (1970), and Hundhausen (1972). Current solar wind research problems are reviewed by Holzer (1978) and Hollweg (1978).

Some observational information is presented in this review, but more comprehensive discussions of observational data are contained in the reviews by Conti (1978) and Reimers (1975, 1978) for early- and late-type stars, respectively. The effect of the mass loss by stellar winds on stellar evolution is studied by Chiosi, Nasi & Sreenivasan (1978), and the effects of a wind on the surrounding interstellar medium are studied by Weaver et al. (1977).

Stellar Wind Theories

Current stellar wind theories fall under three broad classes.

1. Radiative models. For the very luminous stars, radiative acceleration of the matter in the outer atmosphere can occur if there is sufficient opacity at wavelengths near flux maximum. In early-type stars, transfer of photon momentum to the gas occurs through the opacity of the many strong resonance lines in the ultraviolet. The progressive Doppler shifting of the line opacity into the unattenuated photospheric radiation field can result in a rapid acceleration to very high speeds. For late-type stars, the atmosphere is cool enough for grain formation. The radiative force on the infrared continuous opacity of the grains can drive the dust and surrounding gas outward. Unlike the line driven case the acceleration does not depend on velocity gradients, and, as a result, the rate of acceleration is slower and the terminal velocity is lower.

2. Coronal models. Stars that have convection zones, or some other source of acoustic or mechanical wave energy, are expected to have coronal zones as a result of wave dissipation. The outer atmosphere expands as a wind because of the gas pressure gradient. The process is assumed to be similar to that producing the solar wind. In practice, stellar wind theorists have used only the most elementary formulation of solar wind theory, i.e. they have assumed that the flow is that of a spherically symmetric single fluid, in steady state and with no magnetic field constraints. Processes such as those involving two-fluid flow and coronal hole geometry, which are known to be important in the sun, are not considered for two reasons: (*a*) the observational data are rather primitive compared with those available for the sun; (*b*) the winds have mass loss rates and densities that are orders of magnitude higher than in the sun. As a result, many of the solar phenomena associated with closed magnetic structures and large conductive losses may not be relevent. Since the electron densities

are higher, radiative cooling is enhanced and thus temperature structures quite different from that of the expanding solar corona may be produced.

3. Hybrid models. Because fully radiative models and fully coronal models cannot explain various observations, a third class of model, the hybrid corona-plus-radiatively-driven-wind models, are receiving some attention. For example, Hearn (1975a) has shown that the density in the flow from an OB supergiant is so large ($\sim 10^{10}$ cm^{-3} at $2R_*$) that rapid cooling of a coronal gas should occur. The temperature should drop rapidly in a "recombination region" at a height where mechanical deposition ceases to be effective. He suggested the flow is initiated by gas pressure gradients in the corona and is then accelerated to large velocities by the line acceleration mechanism, which is effective beyond the recombination regions. For the winds from the cool stars, Kwok (1975) appealed to turbulence in the chromospheric region to enhance the density at the dust condensation zone. Thus far, the hybrid models have been pursued primarily from a semiempirical standpoint. Cassinelli (1979) describes several studies to test the observational consequences of the hybrid model of Hearn (1975a). These studies are discussed in Section 3. Studies of the dynamical properties of the corona-plus-radiative-wind models will most likely be an active area of theoretical research in the next decade.

In addition to these three broad classes of theories, several other driving mechanisms have been investigated. The effects of rotation on radiatively driven winds have been studied by Marlborough & Zamir (1975). Belcher & MacGregor (1976) considered magnetically driven winds and the loss of angular momentum during the evolution of stars of spectral type F5 and later.

Stars Having Measured Mass Loss Rates

Many of the stars for which mass loss rates have been estimated are shown in Figure 1. The order of magnitude of the mass loss rate is indicated by the size of the symbols. Pre–main-sequence objects, which have very large mass loss rates for their luminosity, are indicated by the open circles. The mass loss rate estimates shown in the figure were taken from a number of sources. (*a*) For the early-type stars, most of the data for Of and OBA supergiants are available from the infrared survey of Barlow & Cohen (1977). Estimates from radio fluxes are available for P Cygni in Wendker et al. (1975) and for ζ Pup in Morton & Wright (1978). Line profiles were used to derive mass loss rates for τ Sco (Lamers & Rogerson 1978), the Be star ψ Per (Bruhweiler et al. 1978), the Wolf-Rayet star HD50896 (Rumpl & Cassinelli 1979), the central stars of planetary nebulae (Heap 1978), and pre–main-sequence stars (Garrison 1978, Kuhi 1964). (*b*) For the late-type stars, mass loss rates can be estimated from blueward

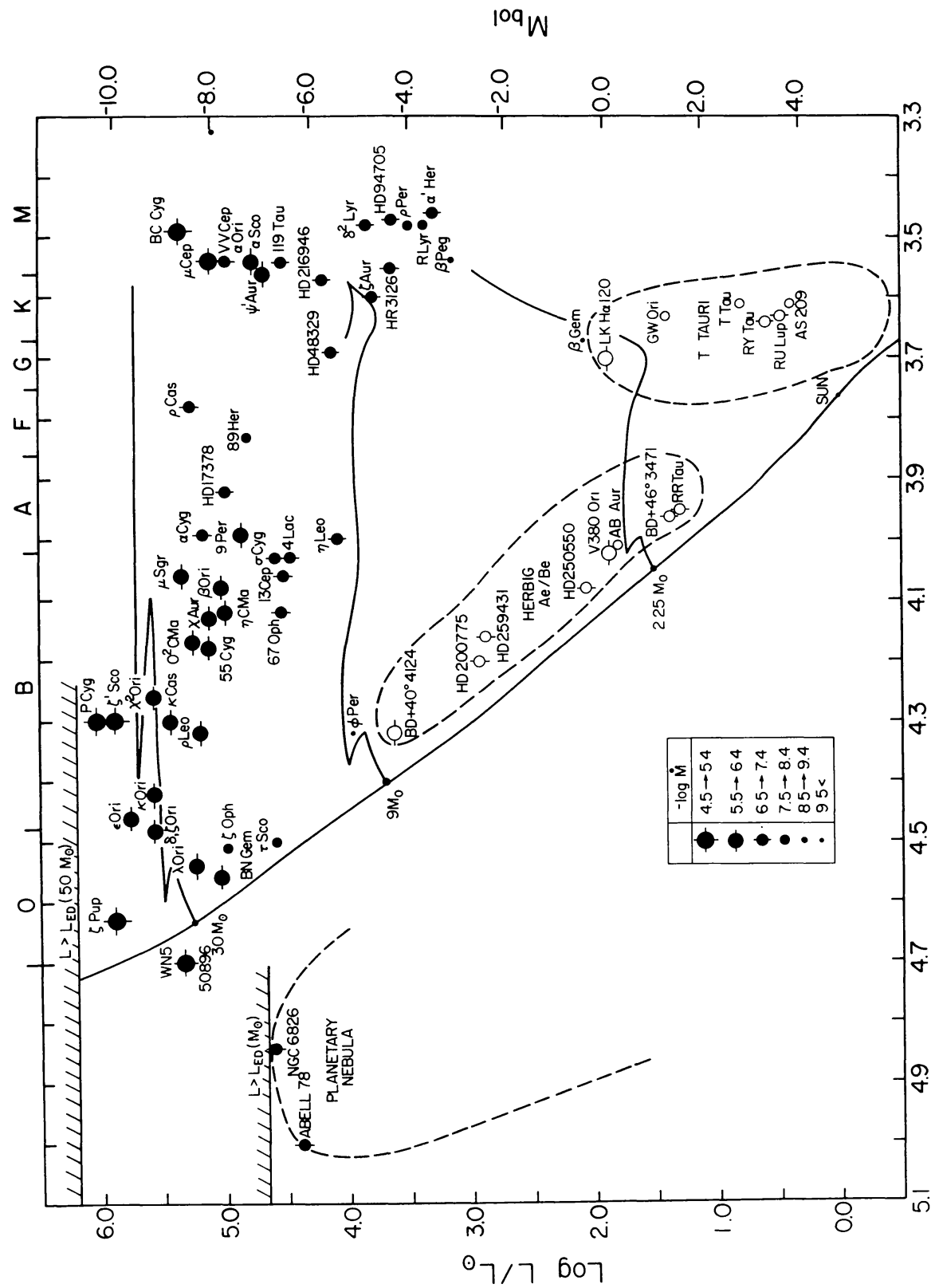

shifted cores in metallic resonance lines (Sanner 1976 and references in Reimers 1975), and from absorption seen in the spectra of a nearby companion (Bernat 1977, Reimers 1977, van der Hucht et al. 1979). The mass loss rate estimates for the late-type stars differ by one to two orders of magnitude, so averages of the logarithm of $\dot{M}$ were used for the estimate shown in Figure 1. The causes for the uncertainties are discussed in Section 4.

Note that most of the data concerning mass loss rates is for luminous stars earlier than about A5 and later than K4. Reimers (1977) completed a survey of stars in the intermediate spectral region and found that there are many stars with evidence for mass loss through shortward displaced absorption features in the cores of the Ca II H and K lines. However, it is difficult to derive reliable mass loss rates from that data alone. These problems are discussed in Section 3.

There are few supergiants of spectral class F and G, presumably because of the rapid evolution through this portion of the H-R diagram. Shown in Figure 1 are estimates for the mass loss rates from ρ Cas and 89 Her. The mass loss from these stars may not be steady but may occur in sporadic mass loss episodes (Sargent 1961, Sargent & Osmer 1969).

As a result of the gap in information concerning mass loss from stars of intermediate spectral type, the subject of stellar winds is currently divided into two parts: (*a*) the winds from hot stars for which radiation pressure on lines plays an important role in the dynamics, and (*b*) the winds from cool evolved stars for which coronae and dust are thought to be important. In Section 2 the basic stellar wind equations are presented, including terms to represent radiative acceleration and radiative and mechanical energy deposition. In Section 3 the winds of hot stars are considered. The theory of line driven winds is discussed, and a graphical solution of the nonlinear momentum equation is presented. Current difficulties with the theory and recent attempts to explain observed ionization anomalies are discussed.

Section 4 is concerned with the winds of cool evolved stars. Both coronal and dust driven models have been considered. Mullan's (1978) application of the Hearn (1975b) minimum energy coronal theory is discussed, as is Mullan's explanation of the locus in the H-R diagram that separates stars with large mass loss rates from those with undetectable

←*Figure 1* Location on the Hertzprung-Russell diagram of stars for which mass loss rates have been estimated. The size of the symbol indicates the magnitude of the mass loss rates in solar masses per year. Pre–main-sequence stars are shown with open circles. Eddington radiative instability limits for stars of 1 and 50 solar masses are indicated by the boundaries of the cross-hatched area. Evolutionary tracks for stars of 2.25, 9, and 30 solar masses are shown.

winds. A wide variety of observational techniques have been used to study the winds and the dust in the wind of the M stars. These techniques are reviewed and the dust driven wind theory is discussed briefly.

2 STELLAR WIND EQUATIONS

Most of the theoretical work thus far on stellar winds assumes a steady, radial, spherically symmetric flow. With these assumptions, the fluid flow equations expressing conservation of the mass, momentum, and energy of the gas may be written as

$$\dot{M} = 4\pi\rho\, vr^2 = \text{const}, \tag{1}$$

$$v\frac{dv}{dr} + \frac{1}{\rho}\frac{dp}{dr} + \frac{GM}{r^2} + g_R = 0, \tag{2}$$

$$v\frac{de}{dr} + p\,v\frac{d}{dr}\left(\frac{1}{\rho}\right) = -\left(\frac{1}{\rho}\right)\left(\nabla\cdot\mathbf{q}\right) = \frac{1}{\rho}\left(Q_A + Q_R - \nabla\cdot\mathbf{q}_c\right), \tag{3}$$

where ρ is the mass density, v is the radial speed, p is the gas pressure, e is the internal energy per unit mass, g_R is the acceleration produced by radiation pressure. The heat added to the gas is represented by the divergence of the energy flux $\mathbf{q}$, and Q_A is the energy deposited per volume by acoustic or mechanical energy, Q_R is the rate of deposition of radiative energy, and $\mathbf{q}_c$ is the conductive flux. The fluid equations, including a thorough discussion of the radiation terms, are derived in Chapters 14 and 15 of the stellar atmospheres text by Mihalas (1978). An elegant formulation of the equations, accounting for both mechanical energy deposition and mass deposition, is given in Holzer & Axford (1970).

The radiative acceleration is proportional to the radiative flux and thus tends to decrease as r^{-2}, as does gravity, g. Hence it is often convenient to use the ratio

$$\Gamma_R = g_R/g, \tag{4}$$

and to separate the radiative acceleration into its continuum and line contributions,

$$g_R = \frac{4\pi}{c}\int_{\nu=0}^{\infty} k_\nu H_\nu d\nu, \tag{5}$$

$$= \frac{k_F L}{4\pi c r^2} + \sum g_l, \tag{6}$$

where k_F is the continuum flux mean opacity (in cm^2/gm) and g_l is the

acceleration due to the lth spectral line. The momentum equation may be rewritten as

$$v\frac{dv}{dr}+\frac{1}{\rho}\frac{dp}{dr}+\frac{GM}{r^2}\left(1-\Gamma\right)+\sum g_l=0, \tag{7}$$

where

$$\Gamma=\frac{k_F L}{4\pi cGM}. \tag{8}$$

In the interior of the star, the net acceleration must be inward; the star is radiatively unstable if the ratio of the radiative acceleration on electron scattering to gravity, Γ_{es}, exceeds unity. This is the "Eddington limit" on the luminosity-to-mass ratio

$$\Gamma_{es}=\frac{\sigma L}{4\pi cGM}\leqq 1, \tag{9}$$

where σ is the electron scattering opacity per gram. The Eddington limits for stars of 1 $M_\odot$ and 50 $M_\odot$ are shown in Figure 1.

The momentum and gas energy equations (2, 3) can be combined in the form:

$$\frac{d}{dr}\left[\dot{M}\left(\frac{v^2}{2}+e+\frac{p}{\rho}-\frac{GM}{r}\right)+4\pi r^2\left|\mathbf{q}_c\right|\right]=\dot{M}g_R+\frac{\dot{M}}{\rho v}\left(Q_R+Q_A\right). \tag{10}$$

Letting E, be the energy per unit mass of the gas

$$E=\left(\frac{v^2}{2}+e+\frac{p}{\rho}-\frac{GM}{r}\right), \tag{11}$$

Equation (7) integrates to give

$$E=E_0+\frac{1}{\dot{M}}\int_{r_0}^{\infty}\left(v\rho g_R+Q_R+Q_A\right)4\pi r^2\,dr+\frac{4\pi}{\dot{M}}\left[r^2\left|\mathbf{q}_c\right|-r_0^2\left|\mathbf{q}_c\right|^0\right]. \tag{12}$$

Thus, even though E is negative deep in the flow it may become positive farther out because of (*a*) deposition of radiative energy, (*b*) deposition of mechanical energy, or (*c*) momentum deposition by radiative acceleration of continuum and line opacity of the gas (Holzer 1977).

The various approximations employed in stellar wind theory can be summarized with reference to Equations (7) and (12).

1. In purely radiatively driven wind theories, it is assumed that there is no mechanical energy deposition, $Q_A = 0$, and that the temperature is

so low that conduction is unimportant, $|\mathbf{q}_c| = 0$. The time required by the material to gain and lose energy is short compared to flow time scales, hence the flow is nearly in radiative equilibrium. In this case the energy of the gas flow is much less than the radiative luminosity $\dot{M}\,E \ll L_*$ and

$$Q_R = \int_0^\infty 4\pi\kappa_\nu\,(J_\nu - B_\nu)\,d\nu \approx 0, \tag{13}$$

where κ_ν, the absorptive opacity, and J_ν, the mean intensity, are evaluated in the frame moving with the fluid (Castor 1972, Cassinelli & Castor 1973, Mihalas 1978). The radiative equilibrium condition, (13), can be used to derive the temperature distribution in the flow using temperature correction procedures if the wind is very thick, as in Wolf-Rayet stars (Cassinelli & Hartmann 1975) or in massive M supergiant flows (Menietti & Fix 1978). More commonly, it is assumed that the flow is isothermal with a temperature that is appropriate for a gas in radiative equilibrium (Klein & Castor 1978):

$$T_e \approx 0.8\,T_{\text{eff}}. \tag{14}$$

For the isothermal case, Equation (7) has the form

$$\frac{r}{v}\frac{dv}{dr} = \left[2a^2 - \frac{GM}{r}\left(1-\Gamma_R\right)\right] \Big/ \left(v^2 - a^2\right), \tag{15}$$

where a is the isothermal sound speed ($a^2 = RT$). Assuming for the moment that g_R does not depend on dv/dr, then this equation has the quotient form that is familiar from solar wind and de Laval nozzle theory (Brandt 1970). For transonic flow to occur it is necessary that the numerator vanish at the sonic point where $v = a$. Marlborough & Roy (1970) and Cassinelli & Castor (1973) discuss constraints on Γ_R to permit transonic flow: Γ_R must be less than unity at and below the sonic point in order for the velocity gradient to be positive. Beyond the sonic point, Γ_R may be larger than unity and large velocity gradients may be produced in the supersonic region. Equation (13), or a slight variant of it, was used by Lucy & Solomon (1970) for line driven winds, by Cassinelli & Hartmann (1975) for continuum driven winds of hot stars, and by Kwok (1975) and others for dust driven winds. In each of these cases, Γ_R was sufficiently close to unity at the sonic point that transonic flow could occur in a *cool* gas. That is, the effective escape speed $2GM(1-\Gamma_R)/r$ is small and therefore the numerator of (13) can vanish for small a. For dust driven winds, Γ_R increases rapidly to near unity in the dust condensation region.

A quite different form of the momentum equation is considered in the line driven theory of Castor, Abbott & Klein (1975), who explicitly accounted for the dependence of the line force on dv/dr. In their theory $\sum g_l \propto (dv/dr)^{\alpha}$ where $\alpha \sim 0.7$ so the momentum equation is not linear and the topology of the solution is greatly different from the familiar X-type singularity associated with (15). This solution is discussed in Section 3.

2. In coronal wind models, it is common to assume that the energy deposition occurs in a thin shell at the base of the flow and to consider only the solution beyond that region, where $Q_A = 0$. For hot coronae, radiative heating by absorption is negligible, but significant radiative cooling can occur by recombination or through collisionally excited line radiation, so $Q_R = N_e{}^2\Lambda$, where $\Lambda(T)$ is the cooling function (Cox & Tucker 1969). The spatial distribution of the mechanical deposition is unknown. Hearn proposed a "minimum flux coronal model" in which the pressure and temperature at the base of the corona are determined if the magnitude of the total mechanical deposition, i.e. $\int Q_A\, dV$, integrated over the volume of the corona, is known. This model is discussed in Section 4.

3. In the hybrid models such as the corona-plus-cool-wind model of Hearn (1975a) and Cassinelli & Olson (1979), constraints on the coronal emission measure $\int N_e^2\, dV$ and hence on $\int Q_A\, dV$ can be derived from the requirement that the X-ray emission account for the anomalous ionization seen in the wind and that X rays satisfy observational limits. Details of the transition to the line driven flow have not been worked out, however it is probably adequate to assume that $Q_A = 0$ in the transition, that Q_R is the dominant energy loss term, and that the radiative acceleration increases rapidly in the recombination zone.

3 STELLAR WINDS OF EARLY-TYPE STARS

Observations

Winds from early-type stars are detected through the presence of broad P Cygni-shaped profiles, and are characterized by large mass loss rates, 10^{-8} to 10^{-5} $M_\odot$/yr, and by large flow velocities, 600 to 3500 km/sec. Although ground-based observations of emission lines in O and B supergiants indicated expanding atmospheres, not until the rocket-ultraviolet observations of Morton (1967) and his collaborators (Morton, Jenkins & Brooks 1969) was the extreme nature of the winds realized. Observations of the winds and the effects of mass loss on stellar evolution are described by Snow & Morton (1976), Conti (1978), and Hutchings (1978).

In the past few years a significant amount of data concerning mass loss

rates, terminal velocity, and ionization conditions have been derived as a result of the completion of extensive surveys of the infrared continuum and ultraviolet line spectra.

1. Barlow & Cohen (1977) derived mass loss rates from their infrared continuum photometry of 44 early-type stars. They found that the mass loss rates are nearly proportional to the stellar luminosity ($\dot{M} \propto L^{1.1}$) and only slightly dependent on the effective temperatures of the supergiants. Mass loss rates can be derived from the long wavelength continua because the free-free opacity increases as λ^2, and at sufficiently long wavelength, optical depth unity occurs in the wind itself. Radio observations provide the most accurate method of determining mass loss rates, because the flux originates far enough out in the flow that the gas has reached terminal velocity, and the flux is nearly independent of the temperature in the flow. Radio fluxes have been used to derive $\dot{M}$ for only a few stars (Morton & Wright 1978) and much more information is expected in the future from VLA radio observations. The theory for deriving $\dot{M}$ from free-free continuum observations is given by Wright & Barlow (1975), Panagia & Felli (1975), and Cassinelli & Hartmann (1977).

2. The richest sources of information concerning the winds of hot stars are the accurate line profiles obtained from Copernicus. The P Cygni profile of OVI in ζ Pup is shown in Figure 2 (Morton 1976). The Copernicus spectra of 60 O and B stars are given in the catalogue of Snow & Jenkins (1977). The terminal velocities of the winds can be derived from the strongest P Cygni profiles if they have a vertical short wavelength edge to their absorption components. Abbott (1978a) derived an

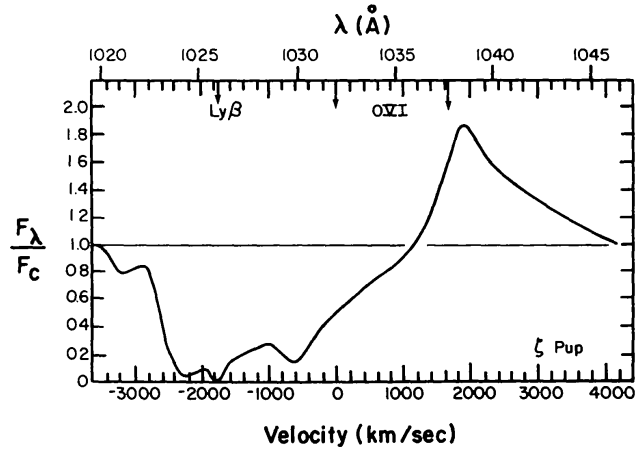

Figure 2 P Cygni profile of the OVI $\lambda\lambda$1031.945, 1037.619 lines in the spectrum of ζ Pup (O4f) Morton (1976). The arrows indicate the rest wavelengths of the lines. The velocity scale at the bottom gives the Doppler displacement from the 1031.9-Å component. The core of the stellar Lyman β line is seen at -1900 km/sec. Interstellar lines have been eliminated.

empirical relation between terminal speed and photospheric escape speed, $v_\infty = 3\, v_{esc}$, for 34 O, B, A, and Wolf-Rayet stars.

3. Copernicus spectra can also be used to derive the relative abundance of various ionization stages of a given element and to provide some information on the velocity structure of the winds (Lamers & Morton 1976). Extensive families of theoretical P Cygni profiles were recently calculated (Olson 1978, Castor & Lamers 1979). Thus, good estimates of the ionization structure for the large number of hot stars may now be derived. The Copernicus spectra show strong lines of anomalously high stages of ionization, such as OVI in supergiants as late as B0.5Ia, and Si IV as late as B8I. Summaries of these anomalies along with two quite different explanations are presented by Lamers & Snow (1978) and Cassinelli & Olson (1979). The discovery of the high stage of ionization led to the realization that mechanical energy deposition occurs somewhere in the flow and revived interest in chromospheric and coronal models of the winds such as those proposed by Cannon & Thomas (1977) and Hearn (1975b).

Wind Models

Recent theoretical work has proceeded along two lines.

1. A purely radiatively driven wind theory has been developed by Castor, Abbott & Klein (hereafter CAK 1975, 1976). The high velocities and large mass loss rates are produced by the transfer of momentum from radiation to the gas, by way of line opacity. Abbott (1977, 1978b) and Castor (1978) recently refined the theory to include a large number of lines and a more accurate treatment of the radiation transfer in lines. The energy equation is not treated explicitly because there are a sufficient number of strong lines to drive the winds, even if the gas temperature is only roughly that which is expected in radiative equilibrium. The theory does not explain the ionization anomalies such as OVI.

2. In the development of empirical models, efforts have been made to derive the temperature and velocity structure of the winds from the observed line profiles and continuous energy distributions. Several models proposed to explain the observed ionization anomalies are presented in a review by Cassinelli, Castor & Lamers (1978). The models start with an assumed temperature and velocity structure, and then observational consequences are derived from theoretical calculations of optical and ultraviolet line profiles, and of calculations of continuum fluxes from X-ray through radio wavelengths. Lamers & Morton (1976) exposed several deficiencies in the line driven wind theory from such a process. Van Blerkom (1978) found from a study of Balmer line profiles that the velocity distribu-

tions in hot stars tend to be of two types, either "rapid accelerators," such as the winds of O stars, or "gradual accelerators," such as the massive wind of P Cygni.

Line Driven Wind Theory

A photon that is emitted from the photosphere at a frequency larger than that of a strong line may become resonant with that line opacity in a shell somewhat higher in the atmosphere, if the outer layers of the atmosphere are accelerating in the outward radial direction. If ν is the original frequency of the photon and ν_0 is the line central frequency, then the shell at which the photon may be scattered occurs where the flow velocity has reached the value

$$v(r) = c(\nu - \nu_0)/\nu_0.$$

The transfer of radiation through the shell is adequately described by the Sobolev escape probability theory (Sobolev 1960, Castor 1970, Mihalas 1978). Although a photon may scatter many times within the shell, the net momentum and the net energy imparted to the shell depend on the angle at which the photon leaves the shell after its last scattering.

The maximum mass loss rate that can be produced by one strong line, as for example the Lucy & Solomon (1970) case, can be derived by equating the final mass momentum flux $\dot{M}v_\infty$ to the photon momentum that is transferred by scattering all the stellar radiation between ν_0 and $\nu_0 + \Delta\nu_{\max}$, where $\Delta\nu_{\max} = \nu_0 v_\infty/c$. Thus,

$$\dot{M}v_\infty = \frac{L_\nu \Delta\nu_{\max}}{c} = \frac{L_\nu \nu_0}{c}\frac{v_\infty}{c},$$

and if ν_0 is near the maximum of the stellar continuous energy distribution, this gives

$$\dot{M} \approx L/c^2. \tag{16}$$

Now if the entire spectrum is covered by nonoverlapping lines, i.e. adjacent lines separated by displacement v_∞, the "single scattering" maximum mass loss rate can be derived from the momentum flux of the entire stellar luminosity, $\dot{M}v_\infty = L/c$, giving

$$\dot{M}_{\max} = L/v_\infty c. \tag{17}$$

This is a factor c/v_∞ (i.e. $\sim$100) greater than that of Equation (16). For $L = 10^6\ L_\odot$, $v_\infty/c = 0.01$, Equation (17) gives $\dot{M}_{\max} = 7 \times 10^{-6}\ M_\odot$/yr, just about the mass loss rate observed from the most luminous Of and W-R stars and OB supergiants. The final kinetic energy luminosity of the star is, from Equation (17),

$$\frac{1}{2}\dot{M}\, v_\infty^2 = \frac{1}{2}\left(\frac{v_\infty}{c}\right) L, \tag{18}$$

or only about 0.5% of the radiative luminosity. So, although each photon has been scattered by one shell, it has not been destroyed. The photons have been redshifted by as much as $v_0 v_\infty/c$ and, except for the photons that are scattered back into the photosphere, they are seen as the "emission component" of the P Cygni profile, and as the residual radiation in the core of the P Cygni absorption component.

A photon that escapes from the resonant shell of one line may encounter another shell where it is resonant with a different line. Rybicki & Hummer (1978) developed a generalized form of the Sobolev theory to treat the problem of multiple resonance shells. Castor (1978) discusses the effects of multiple scattering on the flow dynamics and indicates that the extra momentum that can be imparted will not raise the maximum mass loss rate to more than about a factor of two or three above that given in Equation (17).

The acceleration imparted to a shell as a result of resonance line scattering of photospheric radiation is given by Lucy (1971) and Castor (1974). If πF_ν is the radiative flux incident on the innerside of a shell that has a line opacity resonant to photons of frequencies $\nu \pm \Delta\nu_D/2$, then the radiative acceleration of the shell is

$$g_L = \kappa_L \frac{\pi F_\nu}{c} \Delta\nu_D \frac{[1-\exp(-\tau_L)]}{\tau_L}, \tag{19}$$

where κ_L is the opacity (cm^2/gm) at line center; $\Delta\nu_D = \nu_0\, v_{th}/c$, where v_{th} is the thermal velocity of the absorbing ion. The quantity τ_L is the effective optical thickness of the expanding shell and is given approximately by

$$\tau_L = \kappa_L\, \rho v_{th} \frac{dv}{dr}. \tag{20}$$

In Equation (19), τ_L/κ_L is the amount of mass in a column that can scatter the photons in $\Delta\nu_D$, and $1-e^{-\tau_L}$ is the probability that scattering actually occurs. In two limiting cases we have for strong lines,

$$g_L = \frac{\pi F_\nu}{c} \frac{\Delta\nu_D}{\rho v_{th}} \frac{dv}{dr} \qquad \tau_L \gg 1, \tag{21}$$

and for weak lines,

$$g_L = \frac{\pi F_\nu}{c} \Delta\nu_D \kappa_L \qquad \tau_L \ll 1. \tag{22}$$

Note that the acceleration on strong lines is independent of the line strength, and thus the total acceleration due to strong lines is simply proportional to the *number* of strong lines. Abbott (1977) showed that the 18 most abundant elements have lines that can contribute to this number, and hence extensive line lists must be considered. The force on strong lines depends on dv/dr because a velocity gradient allows a line to move out from behind its own "shadow" and into frequencies where there is a strong continuum flux.

For realistic cases it is necessary to consider lines from many different elements and with a wide range in line strengths. It is, therefore, convenient to define a depth scale independent of line opacity;

$$t = \sigma \rho v_{\mathrm{T}} \Big/ \frac{dv}{dr}, \tag{23}$$

where σ is the electron scattering opacity, v_{T} is the thermal speed of some reference ion, say oxygen, with mass m_{o}. Letting $\eta_i = \kappa_i/\sigma$ and $\mu_i = (m_{\mathrm{o}}/m_i)^{1/2}$ where κ_i and m_i are the opacity and mass of the ion producing the ith line, then the total line acceleration is

$$G_{\mathrm{L}} = \sum_i (g_{\mathrm{L}})_i = \left(\frac{\pi F}{c}\right) \sum_i \frac{F_\nu^i}{F} \eta_i \mu_i \Delta v_{\mathrm{T}} \left(\frac{1 - \exp(-\eta_i \mu_i t)}{\eta_i \mu_i t}\right), \tag{24}$$

$$\approx \frac{\pi F}{c} \sigma \sum_i \frac{F_\nu^i}{F} \Delta v_{\mathrm{T}} \min\left(\frac{1}{t}, \eta_i \mu_i\right). \tag{25}$$

The coefficient of the summation is the radiative acceleration on electron scattering opacity, and the sum is referred to by CAK as "the radiation force multiplier."

$$M(t) = \sum_{\tau_i > 1} \frac{F_\nu^i \Delta v_{\mathrm{T}}}{F} \frac{1}{t} + \sum_{\tau_i < 1} \frac{F_\nu^i \Delta v_{\mathrm{T}}}{F} \frac{\tau_i}{t}. \tag{26}$$

This shows that if there were only strong lines the force multiplier would be proportional to t^{-1} and therefore depend linearly on dv/dr. The force due to strong lines is proportional to the number of strong lines $N(t)$. This number depends on the magnitude of t and on the distribution function giving the number of lines as a function of line opacity $f(\eta_i)$.

Using extensive lists of line strengths to give $f(\eta_i)$, Abbott (1977) found that the number of optically thick lines as a function of t can be fitted by $N(t) = N_0 t^\gamma$ where $N_0 \approx 10^3, \gamma \sim 0.2$ for flow from O stars with $T \sim 30{,}000$ K, and $N_{\mathrm{e}} \simeq 10^{11}$ cm^{-3}. Thus, a realistic mixture of line opacity introduces a further dependence on t. CAK represented the radiation force

multiplier by a fit of the form,

$$M(t) = k\, t^{-\alpha}, \tag{27}$$

and α is determined by the line mixture, ($\alpha \approx \gamma - 1$), and k is the "force constant." If all lines are thick $\alpha = 1$, if all lines are thin $\alpha = 0$. The value of α is an indicator of the fraction of the force that is produced by thick lines, and at very large distances α must drop to zero, where the last strong line becomes optically thin. Incorporating G_L into the momentum equation,

$$v\frac{dv}{dr} + \frac{1}{\rho}\frac{dp}{dr} + \frac{GM}{r^2}(1-\Gamma) - \frac{GM}{r^2}\Gamma\, M(t) = 0, \tag{28}$$

and assuming the flow is isothermal with the sound speed $a = (RT)^{1/2}$, and substituting

$$u = -\frac{2\,GM(1-\Gamma)}{a^2 r} = \frac{v_{esc}^2(r)}{a^2}, \tag{29}$$

$$w = v^2/a^2, \tag{30}$$

$$w' = \frac{dw}{du}, \tag{31}$$

the momentum equation becomes

$$\left(1 - \frac{1}{w}\right)w' + \left(1 + \frac{4}{u}\right) - C(w')^{\alpha} = 0$$

$$= F(u,w,w'). \tag{32}$$

This is the basic equation of the CAK theory. The constant, C, depends on k and the mass loss rate,

$$C = k\left(\frac{\Gamma}{1-\Gamma}\right)^{1-\alpha}\left(\frac{L/c}{\dot{M}v_T}\right)^{\alpha}. \tag{33}$$

Graphical Solution of the Castor, Abbott, and Klein Equation

Equation (32) reduces to the more familiar Parker solar wind equation for $C = 0$. In that simpler case, the equation is linear in w' and has a singularity at the sonic point ($w = 1$). The X-type singularity and the topology of the solutions, $v(r)$, are discussed in Holzer & Axford (1970).

As it stands, Equation (32) with $C \neq 0$ is nonlinear, so for a given radial "position," u, and velocity, w, there is not, in general, a unique solution for w'. Therefore, there is no analytic solution for $w(u)$ [or $v(r)$].

It is possible, nevertheless, to develop considerable insight into the line driven wind theory by considering a graphical solution of Equation (32). For this purpose it is sufficient to consider k and α to be constants, independent of radius. Following Abbott (1977), Equation (32) can be solved for some given (u,w) as follows. Let

$$F = F_1 - F_2 = 0, \tag{34}$$

$$F_1 = (1-1/w)w' + \left(1+\frac{4}{u}\right), \tag{35}$$

$$F_2 = C(w')^{\alpha}. \tag{36}$$

F_1 is linear with respect to w'. Its slope is determined by w and its intercept is determined by the radial variable u. Several examples of F_1 are shown in Figure 3. The function F_2 is also plotted in Figure 3, where it is represented by the dashed line. The intersection(s) of the two functions F_1 and F_2 is the solution(s) for w'. There can be no solution, one solution, or two solutions, and in the latter case they will be called the "leftward" and "rightward" solutions.

Line A shows the function F_1 at small r where the flow is subsonic; note there is one solution for w'. As we integrate $w'(u)$ outwardly from deep in the subsonic region, there continues to be a unique solution for

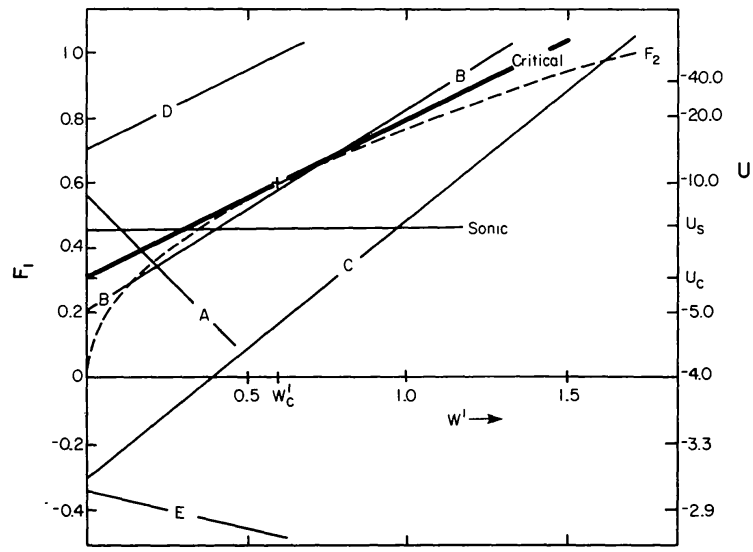

Figure 3 Graphical solution of the CAK equation of motion [Equation (32)]. The curved dashed line shows F_2 (w'). The solid straight lines indicate several forms of F_1 (u, w, w'). The slope of F_1 is determined by w, and the intercept of F_1 is determined by u. The scale on the right-hand side shows values of u corresponding to the intercepts on the F_1 scale. The graphical solution of the equation of motion for w' is the intersection of the line F_1 with the curve F_2.

w' until the sonic point is reached. As seen in the figure there may be two solutions for supersonic flow, and in order for w' to be continuous just beyond the sonic point it is necessary to choose the leftward root for w'. As the speed of the flow increases and the slope of F_1 increases it is possible for F_1 and F_2 to become tangential, i.e.

$$\frac{dF_1}{dw'} = \frac{dF_2}{dw'}. \tag{37}$$

For the solution to continue to higher speeds a regularity or critical point condition must also hold,

$$\frac{\partial F}{\partial u} + \frac{\partial F}{\partial w} w' = 0. \tag{38}$$

Beyond the critical point there are again two solutions (line B), but now the rightward root is the value of w' that will lead to large velocities at large r, where there is again only one solution for w' (line C). Also illustrated in Figure 3 are two cases for which there are no solutions, D and E, indicating that there are no solutions for supersonic flow at small r or for subsonic flow at very large r.

The graphical solution just described was carried out for the case $\alpha = 0.5, C = 0.76, v_{\rm esc}(R_*) = 4.9$. These parameters are chosen for illustrative purposes, and not because they are realistic. The $\alpha = \frac{1}{2}$ case is especially simple because Equation (32) can be transformed into a quadratic equation for w'.

The plot of the numerical solution for v vs r is shown in Figure 4. The regions labeled A to E correspond to the lines with the same letters in Figure 3. Dashed lines in Figure 4 correspond to leftward intercept solutions for w', and solid lines correspond to rightward solutions. There are two solutions for every point in region B. The solutions have a cusp at the intersection with region D. Two cusps join only at the critical point and this allows a continuous transition from low speed to high speed flow.

Unlike the Parker solar wind equation there is no singularity at the sonic point, as can be seen directly from Equation (32). Abbott (1977) demonstrated that the critical point had several of the characteristics of the Parker sonic point. 1. The solution that passes the critical point is the only one that goes smoothly from low subsonic speeds near the surface of the star to high supercritical speeds far away from the star. This is analogous to Parker's unique solar "wind" solution that goes to supersonic speeds far from the star. 2. The presence of the radiation force modifies the speed of propagation of a disturbance, and the critical point

occurs where the flow velocity equals the disturbance speed. Therefore in direct analogy with the Parker sonic point and with the "throat" of a de Laval nozzle, Abbott (1977) finds that "the critical point...(is) the point farthest downwind which is still able to communicate information to all parts of the flow."

Unlike the Parker case, there are no smooth transitions to decelerating (or breeze) flows. The radiation force is always in the outward direction and it therefore depends on the absolute value of w'. Thus, if the negative w' axis were shown in Figure 3, there would be a cusp in F_2 at $w' = 0$, and the only transitions to decelerating flow would have discontinuous velocity gradients. Only positive slopes are shown in Figure 4.

Now consider some prediction that can be made from the line driven theory. From the critical point conditions [Equations (34), (37), and (38)], several useful relations can be derived. Restricting attention to the CAK case for which $v_{esc} \gg a$ and for which the critical point, u_c, satisfies

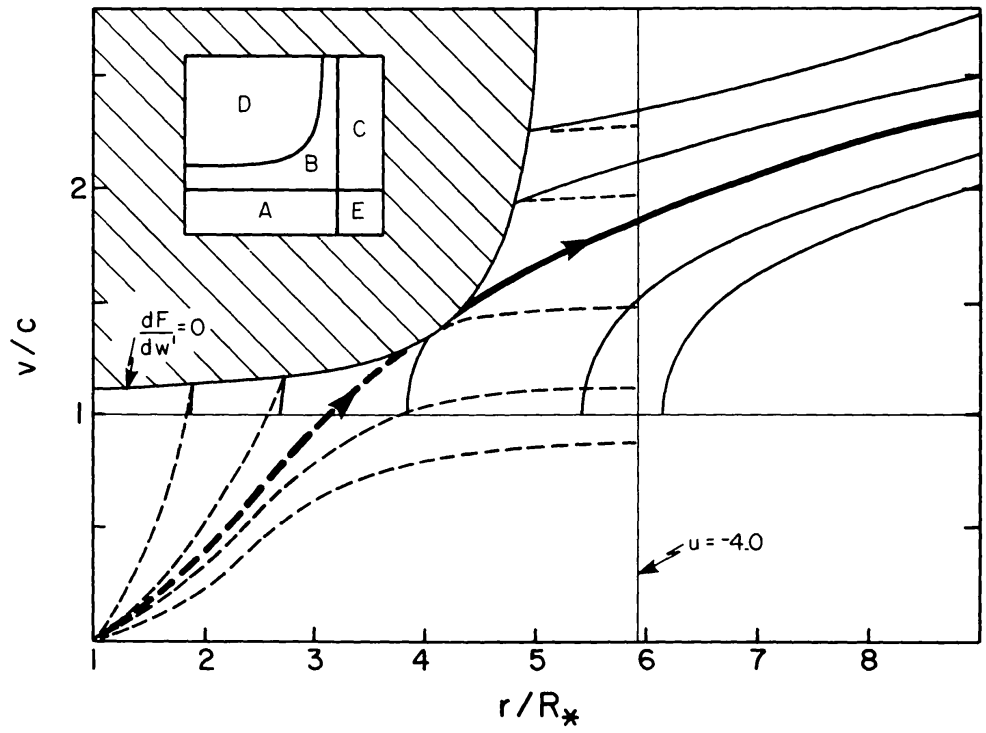

Figure 4 Topology of solutions to the equation of motion for line driven winds in a velocity versus radial distance plane with velocity given in units of the sound speed. The insert identifies regions in the plane, and the letters correspond to the graphical solution shown in Figure 3. In region B there are two solutions for the velocity gradient at any given v and r and these correspond to the case of two intersections of F_1 and F_2 in Figure 3. Dashed lines show results of integrations using the leftward solution for w' and solid lines show the results using the rightward solution. The only solution that goes smoothly from subsonic speeds close to the star to large velocities far from the star is shown by the heavy line.

$4/u_c \ll 1$, we get

$$C = \frac{1}{1-\alpha}\left(\frac{1-\alpha}{\alpha}\right)^{\alpha} \tag{39}$$

$$\dot{M} = \frac{Lk^{\frac{1}{\alpha}}}{v_T c}\left(\frac{\Gamma}{1-\Gamma}\right)\frac{1-\alpha}{\alpha}C^{-\frac{1}{\alpha}} \tag{40}$$

$$v^2 = v_0^2 + \frac{\alpha}{1-\alpha}\frac{2GM(1-\Gamma)}{R_*}\left(1-\frac{R_*}{r}\right). \tag{41}$$

Using these equations, which were derived for the simple case with k and α constant, the theory can explain several of the empirical relations noted earlier. For $\alpha \approx 0.9$, Equations (33) and (39) indicate that $\dot{M} \propto L^{1.1}$, as derived empirically by Barlow & Cohen (1977) from their infrared survey. The terminal velocities are correctly predicted by Equation (40) to scale with v_{esc}, in agreement with the empirical law, $v = 3v_{esc}$, of Abbott (1978a).

More sophisticated versions of the theory recently developed by Abbott (1977) and Castor (1978) provide answers to several questions raised about the original CAK theory. Abbott (1977, 1978c) compiled extensive lists of lines and found that there are enough strong lines available to intercept sufficient flux to account for the observed mass loss rates. Furthermore, Abbott (1978b) derived the extent of a region in the H-R diagram in which the line acceleration in a static atmosphere exceeds gravity at large enough optical depth that the atmosphere must expand. This is a region in which the winds can be "initiated" solely by the radiation mechanism, and it corresponds well to the zone in the H-R diagram where outflows are actually observed. The effect of rotation would be to lower the boundary of the self-initiated wind region so that it includes the Be stars. This indicates that Be star winds should be emanating from a limited equatorial region. Castor (1978) comments on the effects of rotation on line driven winds of the more luminous stars and suggests that the mass loss rate may be the same at the polar and equatorial regions but the rate of increase of velocity is slower in the equatorial regions, leading to a density enhancement there.

While it is now, perhaps, clear that winds can be produced fully by radiative processes, whether or not they actually are is still under contention. Thomas (1978) criticizes the radiatively driven wind models for assuming laminar, steady state flow with a smooth transition to supersonic speeds. He contends that the mass loss is imposed by subphotospheric motions, and as a result, shocks will occur in the flow.

The CAK theory explains the observed mass loss rates and dependence on L and T_{eff}, as well as the magnitude of the terminal velocity. These successes indicate that a major part of the mass loss mechanism has been

identified. However, the presence of OVI in the spectra and the variability of the stellar winds (York et al. 1977, Stalio & Upson 1979) indicate that the picture is far from complete.

Semiempirical Models

The purely radiatively driven wind theory does not consider the possibility that mechanical energy deposition could affect the temperature and the dynamics of the flow. Several semiempirical models have been developed to derive the actual run of temperature in the wind of O stars and B supergiants. Cassinelli, Castor & Lamers (1978) review three quite different models that can explain the high stages of ionization observed in the UV spectra. The models can be used to make other predictions and they can then be refined or rejected on the basis of observational tests.

Lamers & Morton (1976) found that the ionization seen in the ultraviolet spectrum of ζ Pup, ranging from C^{+2} to O^{+5}, is the same as that of an optically thin plasma at $T = 2 \times 10^5$ K. They postulated that the wind has this elevated or "warm" temperature throughout the extended region in which OVI must exist. Lamers & Rogerson (1978) explained the OVI in τ Sco (BOV) by adopting the warm wind model. Lamers & Snow (1978) extended the elevated temperature idea to explain ionization anomalies in B supergiants. Castor, Abbott & Klein (1976) criticized the warm wind model because it ignored the diffuse radiation produced in the wind itself. Cassinelli, Olson & Stalio (1978) criticized it because the model could not explain the strong Hα emission from the winds of Of and OB supergiants. Furthermore, it is difficult to maintain an extended region at a temperature of 2×10^5 K because radiative cooling is especially effective at such temperatures (Cox & Tucker 1969). If the warm temperatures are to be maintained by the deposition of wave energy that emanates from the star, the luminosity of that mechanical energy would have to be about 5% the radiative luminosity of the star, and would have to be deposited over a spatially extended region of several stellar radii.

Castor (1978) found that the ionization could also be explained in a wind at a lower temperature of about 6×10^4 K, if due account was made for the diffuse radiation field in the optically thick winds. This lower temperature satisfies the Hα constraint and requires less energy deposition than a model with $T_e = 2 \times 10^5$ K. However, it does require *some* mechanical energy deposition, and this destroys the aesthetic appeal of the purely radiatively driven wind theory for which no source of energy or momentum deposition is required, other than that of the radiation field of a mechanically quiet star.

An alternative to the elevated wind temperature models is a hybrid model of the type first proposed by Hearn (1975a). Cassinelli, Olson &

Stalio (1978) and Cassinelli & Olson (1979) derived observational constraints on a hybrid corona-plus-cool-wind model from analyses of Hα and ultraviolet profiles and from X-ray upper limits of ζ Pup from the ANS satellite. In this model the winds are cool ($T_e \approx 0.8\ T_{eff}$) as expected from radiative equilibrium, but there is a thin ($<0.1\ R_*$) hot ($T_e \sim 5 \times 10^6$ K) corona at the base of the flow. The high ion stages are produced by the Auger mechanism whereby two electrons are removed from C, N, and O following the K shell absorption of X rays. The mechanical energy deposition required to heat a corona that can produce enough X rays to explain the ionization anomalies is small $\sim 10^{-4}\ L_*$. The model predicts successfully that OVI should persist to B0.5Ia, NV to B2Ia, CIV and Si IV to B8Ia, as is observed. The model also predicts that there will be an emergent 2-keV X-ray flux that is large enough to be detected by the HEAO-2 satellite just recently launched.

Thus, there are at least three very different temperature structures compatible with the observed ionization anomalies, indicating that the ultraviolet resonance lines alone are not accurate indicators of the temperature structure of the winds.

The infrared continuum spectrum, Hα line profiles, and He I lines provide more direct information concerning the temperature of the winds. As discussed by Castor (1978), these depend on both the temperature *and* the velocity distributions in the wind. But fortunately, the emissivities of the IR free-free continuum and the optical line strengths have different functional dependences on T and v, so it should be possible to derive the separated distributions for $T(r)$ and $v(r)$. Cassinelli & Hartmann (1977) and Castor (1978) discuss the effects of temperature rises on the infrared continua of hot stars for a given run of velocity. Cassinelli, Olson & Stalio (1978) and Van Blerkom (1978) studied the dependence of Hα profiles on the velocity structure in winds for a given temperature distribution. However, thus far no complete study of both the IR continuum and Hα profiles has been carried out. None of the three models that explain the ionization anomalies has yet been ruled out. Only after this problem has been settled can we focus attention on the actual source of the mechanical heating.

To summarize, the massive winds of hot stars can be initiated and driven out by radiative momentum transfer alone (Abbott 1978b). However, the discovery of OVI and other high ionization states has led to the realization that there is a source either of mechanical wave energy in the subphotospheric region, or of instability in the flow, that leads to high temperatures. Observations by HEAO-2 and further simultaneous studies of infrared and Hα emission are needed to derive the actual temperature structure in the winds.

4 MASS LOSS FROM EVOLVED LATE-TYPE STARS

Observational Data on Mass Loss

Because of the development of new instrumentation, the number of observational studies of mass loss from cool stars has grown rapidly in the past few years. Surveys of the optical, infrared, and radio spectra are now sufficiently broad that general trends of mass loss rates and wind structures in the H-R diagram are becoming discernable. Some of the particularly useful results are summarized here; more complete reviews of optical, infrared, and radio studies are given by Reimers (1975, 1978), Merrill (1978), and Moran (1976) respectively.

OPTICAL SPECTRA Very high resolution double pass echelle spectrographs were recently used to observe the cores of strong resonance lines and of lines from low excitation levels ($\lesssim 1$ eV) of metals (Bernat & Lambert 1976, Sanner 1976). Superimposed on the photospheric lines are often seen small P Cygni profiles, which, as usual, can be interpreted as having formed in the flow expanding from the star. An example is shown in Figure 5 for Mn I lines in α Ori (M2 Iab). The P Cygni profiles can be analyzed using moving atmosphere radiation transfer techniques to derive column densities, wind velocities, and mass loss rate estimates. Unfortunately,

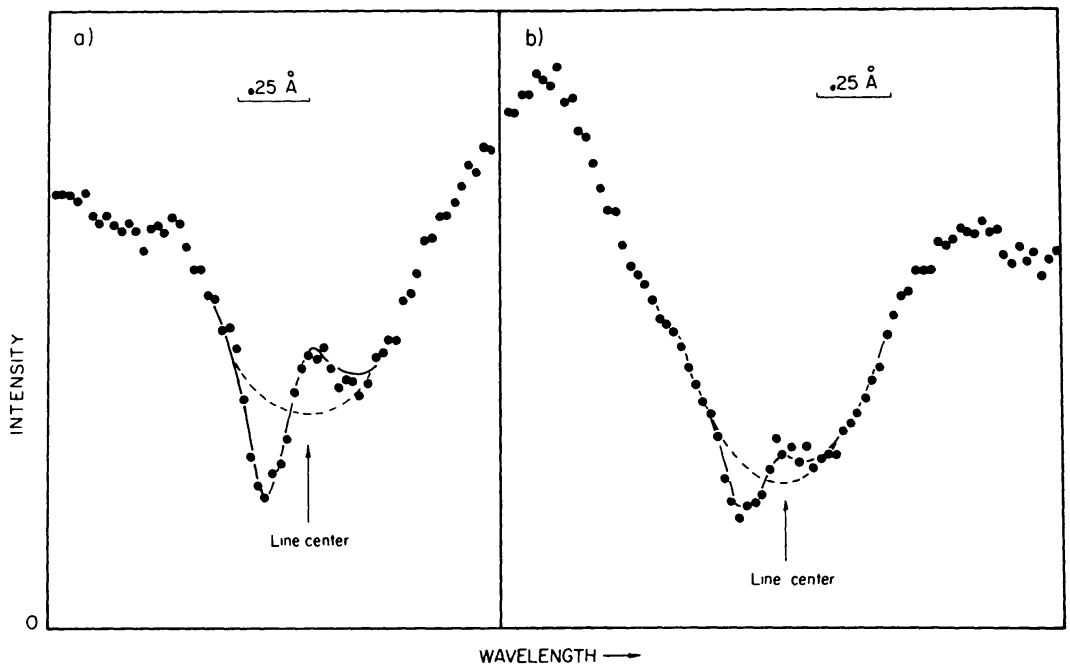

Figure 5 Circumstellar MnI λ4030.8-Å and λ4033.1-Å lines in α Ori, which have P Cygni profiles superimposed upon the background photospheric lines (Bernat & Lambert 1976).

the mass loss rates derived by different authors often disagree by one or two orders of magnitude (Sanner 1976, Bernat 1977, Hagen 1978). This disagreement arises because of the difficulty disentangling the P Cygni lines from the photospheric line, because of the uncertainties in the ionization fraction of the ion producing the line, and, perhaps primarily, because of disagreements as to the "inner boundary" of the line formation region and hence as to the total column mass density in the flow. Reimers (1978) expects the problem to remain unresolved until more UV observations become available and reveal many more resonance lines.

VISIBLE COMPANIONS Another effective way of studying the structure of at least a few cool stars is through analysis of the lines seen superimposed on the spectrum of a near, visible companion. Notable examples of M giants with fainter, hotter companions are α Her (M5 II-III + GO III) and α Sco (M1.5 Iab + B2V). In fact, through a study of α Her Deutsch (1956) was first able to demonstrate that the low velocity flow from M giants actually represents a mass loss. He found that the matter that gave rise to the narrow displaced absorption lines in the spectrum of α^1 Her extended at least beyond the 180 stellar radii to the G companion, and since at that distance the expansion velocity of 10 km/sec was greater than the escape speed, the matter was lost to the interstellar medium. Recently, van der Hucht, Bernat & Kondo (1979) obtained the spectrum of α Sco via the balloon borne ultraviolet spectrometer (BUSS). As additional stages of ionization can be seen in the ultraviolet spectra, these authors were able to derive an improved model for the wind from the M star. They deduced that the entire H II region of the B2 V companion is contained within the cool wind of the M supergiant, 500 AU away, thus illustrating the very extended and massive nature of the outflow. The mass loss rate was derived to be $7 \times 10^{-6}\ M_\odot$/yr; more than an order of magnitude larger than the previous estimates by Sanner (1976) and Kudritzki & Reimers (1978).

INFRARED EXCESSES Extensive surveys of the infrared spectra of luminous cool stars have been carried out since the discovery of the 10-μm silicate feature in μ Cep (M2Ia) and α Ori (M1Ib), and in several Mira variables by Woolf & Ney (1969). The current status is reviewed by Merrill (1978). The strength of the silicate bump can be fitted with theoretical models to derive the column density of the dust and to estimate mass loss rates (Gehrz & Woolf 1971, Hagen 1978). Because there are no sharp spectral features it is impossible to derive, through Doppler shifts, detailed information concerning the spatial distribution of the grains. It is usually assumed that the dust coexists with the gas that produces the P Cygni

features discussed above. Of particular interest to wind theorists is the height above the photosphere at which the grains can form, the condensation radius. It is assumed to be the height at which the grain effective temperature is about 1000 K (Weymann 1978). This radius is very uncertain because it depends on unknown grain properties, such as the absorption coefficient in the near infrared (1–5 μ). Clean silicate grains with a low near-infrared opacity could form rather close to the star. However, observations of the near-IR excess and 10-μm bump indicate the presence of grains having a larger near-IR opacity, as do "dirty grains" (Jones & Merrill 1976) or silicate grains with near-IR band opacity (Hagen 1978). Figure 6 shows the regions in the H-R diagram where there is evidence for the presence of dust from infrared excesses. Dust is detected in all M supergiants and in M giants later than about M3. Dust is also detected around a few F, G, and K supergiants. However, it is unlikely that the temperatures of the winds around these stars fall below the grain condensation temperature. Stothers (1975) suggests that the infrared excesses in these stars arise in a fossil dust shell formed during a prior M supergiant phase of evolution.

MASER EMISSION Strong maser lines of OH, H_2O, and SiO appear in the radio spectra of many Mira variables and in a few peculiar M supergiants such as VY CMa (Wilson & Barret 1972, Moran 1976, Winnberg 1978). Since the masers are pumped by infrared radiation from dust, the

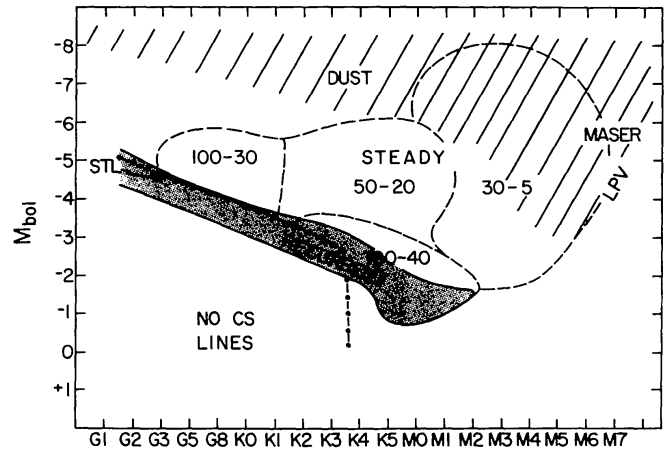

Figure 6 Mass loss domains for late type giants in the H-R diagram (Reimers 1977). At the bottom left-hand side there is no spectroscopic evidence for mass loss from Ca II K circumstellar lines. In the dotted strip, the ejection is recurrent: sometimes shortward shifted lines are seen and sometimes they are not. Above that region the flows are steady. The dashed lines mark various terminal velocity regimes (Reimers 1977, Weymann 1978). Regions in which dust is detected from M stars and from G and K supergiants are indicated. Maser emission is detected from Mira variables and from a few very luminous late M supergiants.

fraction of stars that are maser sources increases with decreasing effective temperature and increasing dust abundance. A good correlation is seen between variable infrared flux and OH maser emission (Moran 1976). Typically the emission due to one transition occurs in two velocity groups, which are displaced by equal amounts to both sides of the stellar velocity. This displacement can be explained by assuming that the maser emission is produced in the extended constant flow velocity regions in the stellar wind, for there is a large correlation path both in front of and behind the star as seen by the observer (Goldreich & Scoville 1976). The displacement of the lines gives the velocity flow. However, since the emission to each side of line center shows multiple velocity groups, the flow is probably clumpy. Furthermore, long baseline interferometer observations show a complicated surface spatial pattern (Reid, Muhlman & Moran 1977). These observations indicate that the simple spherically symmetric, uniform flow picture may be too naive. The major controversy about the winds of cool stars concerns the cause of the flow from the K and early M stars. Unfortunately, these stars do not show maser emission and thus the maser observations are of little help in resolving that problem.

CHROMOSPHERIC EMISSION There is observational evidence for chromospheres in G, K, and early M giants and supergiants from the presence of emission in the cores of the Ca II, H, and K lines (Reimers 1975) and from He I, λ10830 emission in the G and K stars (Zirin 1976). Reimers (1977) finds that stars above and to the right of a sloping line in the H-R diagram have expansion in the chromospheric layers, with speeds as high as one half the terminal speeds. This is seen as a blueward shift of the K_2 emission core and in the K_3 absorption component. Evidence for coronae in a few lower luminosity stars (giants) has been found through UV emission lines of high stages of ionization, such as OV and OVI (Gerola et al. 1974, Dupree 1975, Linsky & Haisch 1979).

Domains of Mass Loss in H-R Diagram

Through a careful analysis of the observational data Reimers (1977) identified several general properties of mass loss from cool stars that can serve as a guide to stellar wind theorists. The range in mass loss rates is roughly 10^{-8} to 10^{-5} $M_\odot$/yr (Figure 1), and mass loss rates tend to increase toward the upper right-hand corner of the H-R diagram. Reimers (1978) gives empirical fit to that trend

$$\dot{M} \simeq 1 \times 10^{-13}\, L/gR, \tag{42}$$

where L, g, and R are the stellar luminosity, surface gravity, and radius in solar units. This relationship can be rewritten as $\frac{1}{2}\dot{M}v_{esc}^2 = 10^{-13}\, L$, and

implies that a constant fraction of the stellar luminosity is being used to provide the necessary energy for escape of the expanding material.

While essentially all M giants and supergiants show evidence for mass loss through the displaced narrow absorption in resonance line cores, the same is not true for the G and K stars. Reimers (1977) finds that these stars fall into two major mass loss domains, depending on whether the displaced Ca K absorption lines are either visible in the spectrum at all times or never visible. The separation between these two is surprisingly sharp, with a third minor group between them in which the lines are sometimes seen and sometimes not. The mass loss domains are shown in Figure 6. Also indicated in the figure is the not particularly uniform trend of expansion velocities derived from the displacement of the circumstellar lines. For the G and early K stars, it is not at all obvious whether the displacements should be interpreted as terminal velocities of the winds (Reimers 1977) or as the velocity of a shell at the wind interstellar medium interface (Mullan 1978). Assuming the velocities are, in fact, wind terminal speeds, Reimers finds a good correlation with the escape speeds of the stars. The velocities increase from the M supergiants (10 km/sec) through the M giants (25 km/sec) and late K supergiants and K giants (20 and 75 km/sec) to the sun with the relation

$$v_{\text{wind}} \propto v_{\text{esc}}^2, \tag{43}$$

and not linearly as might be expected. As both empirical relations [Equations (42) and (43)] extrapolate moderately well to fit the solar wind ($\dot{M}_\odot = 2 \times 10^{-14} M_\odot$/yr), Reimers suggests that the mass loss mechanism may be similar. However, Weymann (1978) notes several difficulties associated with the application of coronal theory to the M supergiants. In the next sections theoretical discussions are presented for a coronal model of G and K stars, and then for a model for dust driven mass loss of M stars.

Coronal Winds of G and K Stars

A coronal model, somewhat like that for the solar wind, is appropriate for stars not luminous enough for radiation pressure effects to be important or too hot for grain formation.

The nature of the coronal heating mechanism is not known and hence, as Mullan (1978) points out, the discussion of coronal properties must necessarily work within a framework in which neither the source nor the mode of coronal heating need be specified. Hearn (1975b) proposes such a framework in his "minimum flux coronal model."

Hearn considers three major sources of energy loss from a corona and expresses each as a flux away from the base of the corona, where the

temperature and pressure are T_0 and P_0. First, there is a conductive flux, F_c, downward into the chromosphere-corona transition region. He assumes, on the basis of solar structure, that the transition region is at a constant pressure $P = P_0$, and he derives the conductive flux by equating the divergence of F_c to the radiative losses in the transition zone. Second, there is radiative energy lost from the coronal material itself, F_R. This depends on the temperature of the corona and on the density distribution by way of the coronal emission measure (N_e^2 Vol). To derive the emission measure, he assumes the coronae are isothermal and the relative velocity and density structure are known from the Parker solar wind theory (Parker 1958, Hundhausen 1972). Finally, there is the energy flux due to the wind itself, F_w, which again comes from the Parker theory. In this way all of the fluxes are expressed in terms of the two coronal parameters T_0 and P_0. In addition energy balance requires that the sum of the losses $F = F_c + F_R + F_w$, be equal to the energy input, which presumably is generated in some way in subphotospheric regions.

Hearn notes that while the total loss flux, F, is a monotonic function of P_0, it is not monotonic in T_0. For a given base pressure, there is a temperature, $T_{min}(P_0)$, for which the loss flux is a minimum. The minimum occurs because F_R decreases with increasing temperature, while F_w and F_c both increase with temperature. Hearn argues that the corona adjusts itself to the structure that minimizes the loss flux, so that $T_0 = T_{min}$. Hence the coronal structure is completely determined by the magnitude of the mechanical flux that enters from below. He identified three cases where a corona could exist as the input mechanical flux is increased. Class I coronal models are those in which the energy loss is dominated by conduction and radiative losses, with mass loss being relatively unimportant in the energy balance; he offers the solar wind as an example. Class II coronae are those in which most of the energy is lost by radiation and mass loss. Class III are coronae dominated by mass loss only; in such cases the sonic point tends to lie very close to the star.

Although Hearn originally developed the theory to explain the initiation of mass loss in OB supergiants, it has subsequently been used primarily for cooler less luminous objects. Haisch & Linsky (1976) modified the equations somewhat to better account for radiative losses in the supersonic wind and then applied the theory to a study of OVI emission seen in Capella. Mullan (1976) applied it to a wide range of giants and dwarf stars. Hearn & Mewe (1976) and Muchmore & Böhm (1978) used it to interpret X-ray data from the coronae of white dwarfs.

The theory has received criticism on several points, as summarized by Vaiana & Rosner (1978). It has not yet been proven that the minimal loss configuration is in fact required for stability as Hearn suggested. It is

not entirely obvious that the structure is independent of the spatial distribution of the mechanical flux deposition (Endler, Hammer & Ulmschneider 1978). The assumption that the transition region is at a constant pressure is not valid in general (Antiarchos & Underwood 1978), and furthermore the structure of this lower region may be determined by closed magnetic structures, as in the sun (Vaiana & Rosner 1978). Mullan (1978) presents several arguments in defense of the theory; for example, stars that have large mass loss rates probably have a sufficiently large kinetic energy density to avoid significant closure into magnetic structures. It is in the treatment of the transition region that the theory is weakest. The energy deposition required to heat an element of matter to provide for the work done as it moves up through the transition region (enthalpy flux) is not accounted for explicitly. Mullan argues that this problem can be circumvented by considering in the theory only the mechanical flux that actually reaches the corona and by assuming that whatever the mechanical flux is, it must dissipate within the transition region an amount equal to the enthalpy flux generated there. Hearn (1979) is developing a more complete theory and is preparing a rebuttal to the criticism of the original paper.

In spite of the difficulties associated with the model, it is worth considering further, both because of an interesting application to cool stars by Mullan (1978) and because possible improvement of the theory can be seen.

As discussed before, a corona can have one of the three structures depending on stellar parameters such as escape speed and input mechanical flux. Mullan finds that an evolving star should shift from one of these classes to another as it moves toward the red giant stage, and eventually may enter the mass loss dominated category, Class III. Roberts & Soward (1972) pointed out that in stars with hot coronae and low surface gravity, the sonic point could move very close to the surface of the star and the wind would be supersonic essentially throughout the corona. Durney (1973) suggested that the transition to such a fully supersonic structure should be observable through a large increase in mass loss rate, and he derived from theoretical considerations a locus on the H-R diagram above which winds should have this structure and enhanced mass loss. Mullan (1978) calls the winds with negligibly thin subsonic regions and essentially completely supersonic flow "supersonic winds," in contrast with "transonic winds," which have a thicker subsonic region. He calls the locus in the H-R diagram the "Supersonic Transition Locus" (STL), above which the winds are "supersonic" and below which the winds are "transonic." In Durney's original derivation, the STL was approximately a horizontal line at $M_{bol} = -3$, and such a locus does not agree particularly well with

any observational transition locus such as that of Reimers (1977) discussed before.

Mullan (1978) used a semiempirical approach in his derivation of the transition locus. The coronal base pressures, P_0, are determined from observational data, and the coronal temperatures, T_0, are determined from Hearn's minimum flux theory.

Kelch et al. (1978) derived the pressure at the top of the chromospheres, P_{TC}, in a large number of stars from chromospheric emission lines. They found that over a range of three orders of magnitude in surface gravity g, P_{TC} could be represented by a power law of the form $P_{TC} \propto g^{1/2}$. Mullan (1978) assumed that the pressure at the base of the corona is some constant fraction ($\sim 1/6$) of P_{TC}. With P_0 known, the Hearn theory allowed him to calculate T_0, the radius of the sonic point, R_S, and the mechanical flux that enters the corona. He then followed the evolutionary track of a star of mass M, in the H-R diagram, using data for T_{eff} and g from stellar evolution models (Iben 1974). As a star evolves, its radius grows faster than the radial distance to the sonic point. When the two radii, R_S and R_*, are equal, a point on the supersonic transition locus has been found. Other points on the STL are found by considering evolutionary tracks of stars with different masses.

While the formal mathematics of this approach is certainly obvious enough, the physical significance of the STL is not so clear. Mullan suggests the following scenario. Before the onset of the supersonic wind, the expansion is fed by purely coronal gas. When the sonic point overlaps the altitude to which chromospheric spicules can penetrate, there is an essentially discontinuous transition to a state in which the expansion is fed by chromospheric material. Typical coronal temperatures derived along the STL are about 4×10^5 K, and chromospheric temperatures are 8000 K. Thus there can be a jump in the density at the sonic point by a factor of 50 when the throat of the nozzle gains access to chromospheric material. Hence, there will also be a jump in mass loss rate by a factor of 50. This is quantitative restatement of Durney's speculation concerning the effect of the onset of supersonic winds. Mullan offers the following observational support for the idea. (*a*) The STL is found to match, reasonably well, Reimer's boundary of the large mass loss regime (Figure 6). (*b*) Stencel (1978) finds evidence for expansion of chromospheric layers beyond the STL, but negligible expansion prior to it. (*c*) Arcturus lies near the STL and sometimes shows phases of large mass loss rates, enhanced by an order of magnitude or more from the low mass loss rate phase.

Additional support for the presence of a sharp transition locus was recently discovered by Linsky & Haisch (1979) from IUE observations of

transition region lines. High ionization stages, such as NV, CIV are seen in the spectra of stars below the STL, but these are absent above the STL. This perhaps indicates that the size of the transition region is much smaller in the mass loss dominated case.

Mullan derives an expression for the dependence of mass loss rate on stellar parameters (in solar units) for stars beyond the STL.

$$\dot{M} = 1.6 \times 10^{-9} M\sqrt{R} \tag{44}$$

in solar masses per year. This expression shows qualitative agreement with what could be inferred from Figure 1, i.e. increasing mass loss to the upper right-hand corner, but it is functionally quite different from Reimer's expression [Equation (42)]. It also does not extrapolate back to fit the Sun, first because of the jump in density at the STL, and then because in the Hearn theory the mass loss rate decreases rapidly as the sonic point moves outward.

Since the Mullan explanation of the high mass loss regime depends so heavily on chromospheric spicules, it seems that the Hearn and Mullan theories could be greatly improved by incorporating the model of the solar transition region of Pneumann & Kopp (1978). These latter authors discuss the observational evidence for steady downflows in the solar transition region that have a mass flux comparable to the estimated upward mass flux in spicules. Thus the solar wind accepts only a small fraction of the upward spicule mass flux. This fraction presumably increases toward unity as the sonic point moves toward the transition region when the star evolves.

With the abundant observational data now available, the subject of coronal mass loss from cool evolved stars could profit from increased involvement in these studies by solar wind theorists.

Dust Driven Winds

After Woolf & Ney (1969) presented evidence for the presence of dust in the envelopes of red giant stars, it became plausible to attribute the expansion to radiation forces on the dust. Gilman (1972) showed that momentum could be transferred from the radiation field to the gas by grain-gas collisions and subsequent gas-gas collisions. The mechanism has now been investigated in several papers (Salpeter 1974, Kwok 1975, Jones & Merrill 1976, Goldreich & Scoville 1976, Lucy 1976, Menietti & Fix 1978). There are several new features to this type of radiatively driven wind theory: (*a*) grain condensation and growth, (*b*) radiation force on grains and the coupling of grain and gas momenta, and (*c*) the sputtering of grains due to a high grain drift velocity.

In order for mass loss rates of around 10^{-6} $M_\odot$/yr to be produced,

grain condensation must commence at a height in the stellar atmosphere at which the density is still relatively large. For stars of spectral class M3 and later, dielectrics should be able to condense sufficiently close to the star, but for the early M and the K supergiants, the mechanism could be effective only if the atmospheric scale height is increased, say by turbulence (Kwok 1975, Weymann 1978).

After grains start to form and grow, they experience a very large radiative force and are assumed to be accelerated to the (local) terminal drift speed. Under these conditions, the momentum equation for dust simply equates the outward radiative force to the inward drag owing to collisions with gas particles. The momentum equation for the gas has the usual gas pressure gradient, gravity, an almost negligible radiation pressure term, and the outward drag by the dust grains. The last term can be replaced by the radiation force on grains, and thus the total radiation force, say Γ_R, of Equation (15), involves the sum of the grain and gas opacities. As before, the flow must obey the Marlborough & Roy (1970) constraint that Γ_R be less than unity at and below the sonic point, and be greater than unity beyond the sonic point.

In Kwok's theory the total opacity increases very rapidly near the dust condensation radius and the flow is accelerated to supersonic speeds. The drift velocity, v_D, of the grains relative to the gas increases as the matter flows out; $v_D \propto \rho^{-1/2}$. When v_D reaches speeds near 20 km/sec, the collisions with the gas particles are energetic enough for grain destruction to occur by way of sputtering. The acceleration to higher speeds ceases and the gas attains the relatively low terminal velocities of 5–50 km/sec detected in the core P Cygni lines and Maser line separations. If sputtering did not occur the flows would reach speeds of about 100 km/sec. These high speeds are, of course, not acceptable from an observational point of view.

Weymann (1978) and Hagen (1978) discuss several observational objections to the radiatively driven dust mechanism for explaining the flows from M stars. (*a*) If the dust is in the form of dirty silicates or more generally if the grains have significant near-IR absorptive opacity (Hagen 1978), then they cannot form and survive close to the star and push the mass flow off. Kwok (1978) counters this objection with the suggestion that clean dielectric grains form near the base of the flow, but they pick up impurities as they flow out. (*b*) Hagen (1978) argues that if the flows are driven by dust, there should be a correlation between the dust column density as measured by the 10-μ bump and mass loss rate, and she finds none. However, since the mass loss rate estimates continue to disagree by an order of magnitude or more and the nature of the near-IR opacity of grains is so uncertain, the lack of a good correlation is no surprise.

Furthermore, the degree of destruction of grains by sputtering should be considered in such an analysis. (*c*) Reimers (1978) finds evidence for expansion in chromospheric regions, with velocities as high as half the terminal speed, and since grains are not likely to exist in these regions, Hagen argues that dust cannot be responsible for the outflow. However, the dust does not have to "push" all the gas out. If a sufficiently large gas pressure gradient is produced as a result of the lifting of outer layers by way of the radiation process, expansion of the deeper layers will occur. Whether or not this is sufficient has yet to be demonstrated. (*d*) A particularly serious criticism of the model is that low velocity flows with apparently small mass loss rates have been detected in a few metal-poor population II stars, around which dust grains will not form (Hagen 1978). This indicates that the flows would occur even in absence of dust. If that is the case, then it would perhaps be best to consider the process of transferring momentum to the flow via dust opacity as a mass loss "enhancement" mechanism. The eventual solution of this problem is going to require a much better understanding of the transition from the thick chromospheric layers to the cool expanding envelope surrounding the stars.

Acknowledgments

I am grateful to D. Abbott for many useful discussions and to W. Waldron for carrying through the graphical solution of the line driven wind equation of motion and for assistance in the preparation of the review. I am indebted to D. Abbott, J. Castor, and J. Fix for helpful comments on the manuscript, and to many authors for preprints of their research. This work was supported in part by the National Science Foundation under grant AST 76-15448 through the University of Wisconsin.

Literature Cited

Abbott, D. C. 1977. PhD thesis, Univ. Colorado
Abbott, D. C. 1978a. *Ap. J.* 225:893–901
Abbott, D. C. 1978b. In *Proc. IAU Symp. No. 83, Mass Loss and Evolution of O-Type Stars*. In press
Abbott, D. C. 1978c. *J. Phys. B.* 11:3479–97
Antiarchos, S. K., Underwood, J. H. 1978. *Astron. Astrophys.* 68:L19–22
Barlow, M. J., Cohen, M. 1977. *Ap. J.* 213: 737–55
Belcher, J. W., MacGregor, K. B. 1976. *Ap. J.* 210:498–507
Bernat, A. P. 1977. *Ap. J.* 213:756–66
Bernat, A. P., Lambert, D. L. 1976. *Ap. J.* 204:830–37
Brandt, J. C. 1970. *Introduction to the Solar Wind*. San Francisco: Freeman
Bruhweiler, F. C., Morgan, T. H., van der Hucht, K. A. 1978. *Ap. J. Lett.* 225:L71–74
Cannon, C. J., Thomas, R. N. 1977. *Ap. J.* 211:910–25
Cassinelli, J. P. 1979. In *Proc. IAU Symp. No. 83, Mass Loss and Evolution of O-Type Stars*. In press
Cassinelli, J. P., Castor, J. I. 1973. *Ap. J.* 179:189–207
Cassinelli, J. P., Castor, J. I., Lamers, H. J. G. L. M. 1978. *Publ. Astron. Soc. Pac.* 90:496–505
Cassinelli, J. P., Hartmann, L. 1975. *Ap. J.* 202:718–32
Cassinelli, J. P., Hartmann, L. 1977. *Ap. J.* 212:488–93

Cassinelli, J. P., Olson, G. L. 1979. *Ap. J.* 229:304–17
Cassinelli, J. P., Olson, G. L., Stalio, R. 1978. *Ap. J.* 220:573–81
Castor, J. I. 1970. *MNRAS* 149:111–27
Castor, J. I. 1972. *Ap. J.* 178:779–92
Castor, J. I. 1974. *Ap. J.* 189:273–83
Castor, J. I. 1978. In *Proc. IAU Symp. No. 83, Mass Loss and Evolution of O-Type Stars*. In press
Castor, J. I., Lamers, H. J. G. L. M. 1979. *Ap. J. Suppl.* 39:481–512
Castor, J. I., Abbott, D. C., Klein, R. I. 1975. *Ap. J.* 195:157–74
Castor, J. I., Abbott, D. C., Klein, R. I. 1976. In *Physique des Mouvements dans les Atmosphères Stellaires*, ed. R. Cayrel, M. Steinberg. Paris: Cent. Nat. Rech. Sci.
Chiosi, C., Nasi, E., Sreenivasan, S. R. 1978. *Astron. Astrophys.* 63:103–24
Conti, P. S. 1978. *Ann. Rev. Astron. Astrophys.* 16:371–92
Cox, D. P., Tucker, W. H. 1969. *Ap. J.* 157:1157–67
Deutsch, A. J. 1956. *Ap. J.* 125:210–27
Dupree, A. K. 1975. *Ap. J. Lett.* 200:L27–32
Durney, B. R. 1973. In *Stellar Chromospheres*, ed. S. D. Jordan, E. H. Avrett, pp. 282–85. NASA Sp-317
Endler, F., Hammer, R., Ulmschneider, P. 1978. *Astron. Astrophys.* Submitted for publication
Garrison, L. M. 1978. *Ap. J.* 224:535–45
Gehrz, R. D., Woolf, N. J. 1971. *Ap. J.* 165:285–94
Gerola, H., Linsky, J. L., Shine, R., McClintock, W., Henry, R. C., Moos, H. W. 1974. *Ap. J. Lett.* 193:L107–10
Gilman, R. C. 1972. *Ap. J.* 1972. 178:423–26
Goldreich, P., Scoville, N. 1976. *Ap. J.* 205:144–54
Hagen, W. 1978. *Ap. J. Suppl.* 38:1–18
Haisch, B. M., Linsky, J. L. 1976. *Ap. J. Lett.* 205:L39–42
Heap, S. R. 1978. In preparation
Hearn, A. G. 1975a. *Astron. Astrophys.* 40:277–83
Hearn, A. G. 1975b. *Astron. Astrophys.* 40:355–64
Hearn, A. G. 1979. Private communication
Hearn, A. G., Mewe, R. 1976. *Astron. Astrophys.* 50:319–21
Hollweg, J. V. 1978. *Rev. Geophys. Space Sci.* 16:689–720
Holzer, T. E. 1977. *J. Geophys. Res.* 82:23–35.
Holzer, T. E. 1978. In *Solar System Plasma Physics: A Twentieth Anniversary Overview*, ed. C. F. Kennel, L. J. Lanzerotti, E. N. Parker. Amsterdam: North-Holland. In press
Holzer, T. E., Axford, W. I. 1970. *Ann. Rev. Astron. Astrophys.* 8:31–60
Hundhausen, A. 1972. *Coronal Expansion and Solar Wind*. New York: Springer
Hutchings, J. B. 1978. *Earth Extraterr. Sci.* 3:123–34
Iben, I. 1974. *Ann. Rev. Astron. Astrophys.* 12:215–56
Jones, T. W., Merrill, K. M. 1976. *Ap. J.* 209:509–24
Kelch, W. L., Linsky, J. L., Basri, G. S., Chiu, H. Y., Chang, S. W., Maran, S. P., Furenlid, I. 1978. *Ap. J.* 220:962–79
Klein, R. I., Castor, J. I. 1978. *Ap. J.* 220:902–23
Kraft, R. 1967. *Ap. J.* 150:551–70
Kudritzki, R. P., Reimers, D. 1978. *Astron. Astrophys.* 70:227–76
Kuhi, L. V. 1964. *Ap. J.* 140:1409–33
Kwok, S. 1975. *Ap. J.* 198:583–91
Kwok, S. 1978. Private communication
Lamers, H. J. G. L. M., Morton, D. C. 1976. *Ap. J. Suppl.* 32:715–36
Lamers, H. J. G. L. M., Rogerson, J. B. 1978. *Astron. Astrophys.* 66:417–30
Lamers, H. J. G. L. M., Snow, T. P. 1978. *Ap. J.* 219:504–14
Linsky, J. L., Haisch, B. M. 1979. *Ap. J. Lett.* 229:L33–38
Lucy, L. B. 1971. *Ap. J.* 163:95–110
Lucy, L. B. 1976. *Ap. J.* 205:482–91
Lucy, L. B., Solomon, P. M. 1970. *Ap. J.* 159:879–93
Marlborough, J., Roy, J. R. 1970. *Ap. J.* 160:221–24
Marlborough, J., Zamir, M. 1975. *Ap. J.* 195:145–56
Menietti, J. D., Fix, J. D. 1978. *Ap. J.* 224:961–68
Merrill, K. M. 1978. In *Proc. IAU Colloq. No. 42, The Interaction of Variable Stars with their Environment*, ed. R. Kippenhahn, J. Rahe, W. Strohmeier. *Publ. Bamberg Obs.* Bd. xi, No. 121, pp. 446–94
Mihalas, D. 1978. *Stellar Atmospheres*, pp. 511–66, San Francisco: Freeman. 2nd ed.
Moran, J. M. 1976. In *Frontiers of Astrophysics*, ed. E. H. Avrett, pp. 385–437. Cambridge: Harvard Univ. Press
Morton, D. C. 1967. *Ap. J.* 147:1017–24
Morton, D. C. 1976. *Ap. J.* 203:386–98
Morton, D. C., Jenkins, E. B., Brooks, N. 1969. *Ap. J.* 155:875–85
Morton, D. C., Wright, A. E. 1978. *MNRAS* 182:47P–51P
Muchmore, D. O., Böhm, K. H. 1978. *Astron. Astrophys.* 69:113–17
Mullan, D. J. 1976. *Ap. J.* 209:171–78
Mullan, D. J. 1978. *Ap. J.* 226:151–66
Olson, G. L. 1978. *Ap. J.* 226:124–37
Panagia, N., Felli, M. 1975. *Astron. Astrophys.* 39:1–5
Parker, E. N. 1958. *Ap. J.* 128:664–76

Parker, E. N. 1963. *Interplanetary Dynamical Processes*. New York: Interscience
Pneumann, G. W., Kopp, R. A. 1978. *Sol. Phys.* 57:49–64
Reid, M. J., Muhlman, D. O., Moran, J. M., et al. 1977. *Ap. J.* 214:60–77
Reimers, D. 1975. In *Problems in Stellar Atmospheres and Envelopes*, ed. B. Baschek, W. H. Kegel, G. Traving, pp. 229–56. Berlin: Springer
Reimers, D. 1977. *Astron. Astrophys.* 57: 395–400
Reimers, D. 1978. In *Proc. IAU Colloq. No. 42, The Interaction of Variable Stars with their Environment*, ed. R. Kippenhahn, J. Rahe, W. Strohmeier, pp. 559–76
Roberts, P. H., Soward, A. M. 1972. *Proc. Roy. Soc. London Ser. A* 328:185
Rumpl, W. M., Cassinelli, J. P. 1979. In preparation
Rybicki, G. B., Hummer, D. G. 1978. *Ap. J.* 219:654–75
Salpeter, E. E. 1974. *Ap. J.* 193:585–92
Sanner, F. 1976. *Ap. J. Suppl.* 32:115–45
Sargent, W. L. W. 1961. *Ap. J.* 134:142–50
Sargent, W. L. W., Osmer, P. S. 1969. In *Mass Loss for Stars*, ed. M. Hack, pp. 57–63. Dordrecht: Reidel
Snow, T. P., Jenkins, E. B. 1977. *Ap. J. Suppl.* 33:269–360
Snow, T. P., Morton, D. C. 1976. *Ap. J. Suppl.* 32:429–65
Sobolev, V. V. 1960. *Moving Envelopes of Stars*. Cambridge: Harvard Univ. Press
Stalio, R., Upson, W. L. 1979. In *Proc. 4th Int. Colloq. Astrophys., Trieste: High Resolution Spectrometry*, ed. M. Hack. In press
Stencel, R. E. 1978. *Ap. J. Lett.* 223:L37–39
Stothers, R. 1975. *Ap. J. Lett.* 197:L25–27
Thomas, R. N. 1978. In *Proc. IAU Symp. No. 83, Mass Loss and Evolution of O-Type Stars*. In press
Vaiana, G. S., Rosner, R. 1978. *Ann. Rev. Astron. Astrophys.* 16:393–428
Van Blerkom, D. 1978. *Ap. J.* 221:186–92
van der Hucht, K. A., Bernat, A. P., Kondo, Y. 1979. *Astron. Astrophys.* In press
Weaver, R., McCray, R., Castor, J., Shapiro, P., Moore, R. 1977. *Ap. J.* 218:377–95
Wendker, H. J., Smith, L. F., Israel, F. P., Habing, H. J., Dackel, H. P. 1975. *Astron. Astrophys.* 42:173–80
Weymann, R. J. 1978. In *Proc. IAU Colloq. No. 42, The Interaction of Variable Stars with their Environment*, ed. R. Kippenhahn, J. Rahe, W. Strohmeier, pp. 577–90
Wilson, W. J., Barrett, A. H. 1972. *Astron. Astrophys.* 17:385–402
Winnberg, A. 1978. In *Proc. IAU Symp. No. 42, The Interaction of Variable Stars with their Environment*, ed. R. Kippenhahn, J. Rahe, W. Strohmeier, pp. 495–520
Woolf, N. J., Ney, E. P. 1969. *Ap. J. Lett.* 155:L181–84
Wright, A. E., Barlow, M. J. 1975. *MNRAS* 170:41–51
York, D. G., Vidal-Madjar, A., Laurent, C., Bonnet, R. 1977. *Ap. J. Lett.* 213:L61–65
Zirin, H. 1976. *Ap. J.* 208:414–25